Changes in ambient temperature are the prevailing cue in determining *Brachypodium distachyon* diurnal gene regulation

Kirk J-M. MacKinnon[1,2], Benjamin J. Cole[3,4], Chang Yu[1], Joshua H. Coomey[1,5], Nolan T. Hartwick[6], Marie-Stanislas Remigereau[4], Tomás Duffy[4], Todd P. Michael[6], Steve A. Kay[4], Samuel P. Hazen[1,*]

[1]Biology Department, [2]Molecular and Cellular Biology Graduate Program, [5]Plant Biology Graduate Program, University of Massachusetts, Amherst, MA, USA. [3]DOE Joint Genome Institute, Walnut Creek, CA, USA, [4]Department of Neurology, Keck School of Medicine, University of Southern California, Los Angeles, CA, USA, [6]J. Craig Venter Institute, La Jolla, CA, USA.

* corresponding author
hazensam@umass.edu

SUMMARY

- Plants are continuously exposed diurnal fluctuations in light and temperature, and spontaneous changes in their physical or biotic environment. The circadian clock coordinates regulation of gene expression with a 24-hour period, enabling the anticipation of these events.
- We used RNA sequencing to characterize the *Brachypodium distachyon* transcriptome under light and temperature cycles, as well as under constant conditions.
- Approximately 3% of the transcriptome was regulated by the circadian clock, a smaller proportion reported in other species. For most transcripts that were rhythmic under all conditions, including many known clock genes, the period of gene expression lengthened from 24 h to 27 h in the absence of external cues. To functionally characterize the cyclic transcriptome in *B. distachyon*, we used Gene Ontology enrichment analysis, and found several terms significantly associated with peak expression at particular times of the day. Furthermore we identified sequence motifs enriched in the promoters of similarly-phased genes, some potentially associated with transcription factors.
- When considering the overlap in rhythmic gene expression and specific pathway behavior, thermocycles controlled diurnal gene regulation. Taken together, our characterization of the rhythmic *B. distachyon* transcriptome represents a foundational resource with implications in other grass species.

Key words: Circadian rhythms, photocycles, thermocycles, gene expression, Brachypodium distachyon

INTRODUCTION

The external environment that plants experience is acutely variable within a single day. Changes in physiological behavior can reflect a direct and immediate response to stimuli, or an anticipated response for a predictable change in the environment. Both types of responses are adaptive, but there is a distinct advantage to anticipating recurring changes (Green *et al.*, 2002; Michael *et al.*, 2003; Dodd *et al.*, 2005). An endogenous timekeeper, known as the circadian clock, provides the capacity to synchronize behavior with the environment, as well as the means to time seasonal behavior. Plant circadian clock oscillations are created by a set of interconnected transcriptional feedback loops that drive morning- and evening-specific outputs (Nohales & Kay, 2016). Morning expressed Myb transcription factors, CIRCADIAN CLOCK ASSOCIATED 1 (CCA1) and LONG ELONGATED HYPOCOTYL (LHY), form the morning loop and bind to the eveing element sequence in the *cis*-regulatory regions of the *PSEUDO RESPONSE REGULATOR* (*PRR*) gene family, including *TIMING OF CAB EXPRESSION 1* (*TOC1*), and repress their expression (Harmer *et al.*, 2000; Arsovski *et al.*, 2015; Nagel *et al.*, 2015; Kamioka *et al.*, 2016). CCA1 and LHY also repress their own expression in addition to genes encoding *EARLY FLOWERING 3* (*ELF3*), *ELF4*, and *LUX ARRYTHMO* (*LUX*), which make up the evening complex (Nusinow *et al.*, 2011). The PRRs in turn function as repressors of the morning loop and the evening complex, as well as within the PRR family (Pokhilko *et al.*, 2012; Gendron *et al.*, 2012; Huang *et al.*, 2012; Liu *et al.*, 2016). Thus, the morning loop, the evening complex, and the PRRs function primarily as repressors of each other (Pokhilko *et al.*, 2012). Activation within the clock occurs by removing this repression, either indirectly through light-stimulated protein degradation or transcriptional repression of the repressing clock genes, or directly through transcriptional activation.

While the core circadian oscillator can intrinsically function for many days, exogenous inputs, e.g. light, humidity, or temperature, are necessary to maintain clock synchronicity (Nohales & Kay, 2016). Light is perceived and transmitted by multiple distinct families of photoreceptors, including phytochromes (PHY), cryptochromes (CRY), ZTL/FKF1/LKP2 proteins (ZEITLUPE, FLAVIN-BINDING KELCH REPEAT F-BOX, and LOV KELCH PROTEIN 2), phototropins, and the ultraviolet light receptor, UVR8 (Zoltowski & Imaizumi, 2014; Franklin *et al.*, 2014; Casal & Qüesta, 2018). Light-dependent photoreceptor activity, in turn, influences the function of core clock proteins. In the dark, ZTL targets TOC1, PRR5, and CCA1 HIKING EXPEDITION (CHE) proteins for degradation, releasing the repression of the morning-expressed genes, CCA1 and LHY (Más *et al.*, 2003; Lee *et al.*, 2018). Both cryptochrome and phytochrome activities have been implicated in controlling the morning loop function of PRR7 and PRR9 (Farré *et al.*, 2005). Phytochromes can also play a key role in the function of evening complex proteins, with PhyA signaling inducing ELF4 expression, and PhyB signaling modulating PHYTOCHROME INTERACTING FACTOR 4 (PIF4) through ELF3 function (Li *et al.*, 2011; Nusinow *et al.*, 2011; Kolmos *et al.*, 2011). PhyB also interacts with CCA1, LHY, GI, TOC1, and ELF3 proteins (Liu *et al.*, 2001; Yeom *et al.*, 2014). ELF3 represses growth, both directly, through inactivation of PIF4 protein, and in a clock dependent manner, transcriptionally repressing *PIF4* as a component of the evening complex (Nieto *et al.*, 2015). More generally, light influences the expression of numerous genes, namely *CCA1*, *LHY*, *GIGANTEA* (*GI*), the *NIGHT LIGHT-INDUCIBLE AND CLOCK-REGULATED* (*LNK*) and *LIGHT-REGULATED WD* (*LWD*)(Nohales & Kay, 2016). The LWDs themselves bind the promoters of *CCA1*, *PRR9*, *PRR5*, and *TOC1*, inducing their expression (Wang *et al.*, 2011; Wu *et al.*, 2016b). Light also causes daytime expression of the LHY-like Myb transcription factor *REVEILLE* 8 (*RVE8*) and the LNKs, which activate several evening-expressed clock genes (Rawat *et al.*, 2011; Farinas & Mas, 2011; Hsu *et al.*, 2013; Rugnone *et al.*, 2013; Xie *et al.*, 2014). Recently, GI was shown to influence light signaling via direct functional interaction with PIF

proteins, further tightening regulatory control of light on clock-mediated transcription (Nohales *et al.*, 2019). Thus, the integration of light signals is mediated through several points in the circadian clock, namely through the activation of gene expression, degradation of proteins, or PhyB light- and temperature-dependent function. These light-responsive events are necessary to time daily rhythms of gene expression.

Temperature serves as an entrainment cue that has independent and overlapping effects with light input into the clock. The function of phytochromes is temperature-sensitive; thus, they are thermosensors as well as photoreceptors (Franklin *et al.*, 2014). Protein reversion from the active to inactive state, which occurs in the dark, is accelerated by an increase in temperature (Jung *et al.*, 2016; Legris *et al.*, 2016). Interestingly, PhyB protein interacts with the evening-complex protein ELF3, and *elf3* mutants are incapable of thermocycle entrainment (Reed *et al.*, 2000; Thines & Harmon, 2010). Similarly, evening-complex function is temperature-sensitive; direct repression of *PRR7*, *GI*, and *LUX* expression increases as nighttime ambient temperature decreases (Mizuno *et al.*, 2014; Box *et al.*, 2015). The *cis*-regulatory region of *LUX* is directly bound and activated by the cold-responsive transcription factor CBF1 (C-REPEAT/DRE BINDING FACTOR, also known as DREB) (Chow *et al.*, 2014). Many of the CBF downstream targets, such as the *COR* genes, exhibit diurnal and circadian clock regulated expression, peaking at the end of the day (Harmer *et al.*, 2000; Michael *et al.*, 2008b; Chow *et al.*, 2014). The clock in turn gates temperature responsiveness (Lee & Thomashow, 2012). Temperature has also been shown to play a role in post-transcriptional and post-translational regulation of circadian clock components and chromatin state (Kumar & Wigge, 2010; Portolés & Más, 2010; James *et al.*, 2012; Seo *et al.*, 2012; Choudhary *et al.*, 2015; Marshall *et al.*, 2016; Gil *et al.*, 2017). Thus, numerous mechanisms and molecular outcomes of thermocycles are key to adaptive changes and buffering against spurious responses to temperature fluctuations.

Here, we use RNA-sequencing to profile the abundance of *Brachypodium distachyon* transcripts under diurnal and constant conditions. We observed robust oscillations under photocycles, thermocycles, and both photo- and thermocycles combined. Specific biological functions, such as secondary cell wall biosynthesis and DNA replication, were mostly entrained by only one input. The circadian clock regulated a relatively small proportion of transcripts, many of which exhibited an unusually long period in constant conditions. Together with observed patterns of growth, metabolism, and gene expression demonstrate that grasses may be relatively responsive to thermocycles rather than the circadian clock (Poiré *et al.*, 2010; Matos *et al.*, 2014; Müller *et al.*, 2018).

MATERIALS AND METHODS

Plant materials and growth conditions

Bd21 seeds were sterilized as previously described (Weigel & Glazebrook, 2006), stratified at 4 °C for 7 days and sown into 100 mL 1x Murashige and Skoog (MS) medium + 0.8 % agar in Magenta boxes. Seeds were germinated in the dark for 3 days, then transferred to diurnal conditions for 10 days (12 h light, 12 h dark, 28 °C day temperature, 12 °C night temperature). Seedlings were then released into one of four conditions: light:dark hot:cold LDHC (12 h light, 12 °C, 28 h dark, 12 °C), LDHH (12 h light, 12 h dark, continuous 28 °C), LLHC (continuous light, 12 h 28 °C, 12 h 12 °C), or LLHH (continuous light, continuous 28 °C). Light intensity was approximately 50 $\mu mol \cdot m^{-2} \cdot sec^{-1}$. Twelve hours after placing the samples in each condition (the evening of the 10th day, just prior to the anticipated day/night transition), the currently emerging leaf was sampled from at least 3 separate plants, pooled, and frozen in liquid nitrogen. Following this first sample, 13 additional time points (14 in total), were collected, one every 3.5 hours.

RNA sample preparation and sequencing

Total RNA was extracted as previously described (Handakumbura *et al.*, 2018). mRNA was enriched through two rounds of polyA selection using the Dynabeads mRNA Purification kit (ThermoFisher Scientific, Waltham, MA). Illumina stranded, paired-end sequencing libraries were then constructed using the ScriptSeq-v2 RNA-Seq Library Preparation Kit (Illumina, San Diego, CA) following the manufacturer's instructions. Libraries were sequenced at the USC Epigenome Core Facility (HiSeq 2000; 6 samples on 1 lane; paired-end 100 cycles) or the USC Genome Core Facility (Hiseq 2500; 42 samples on 7 lanes; 6 samples per lane; paired-end, 100 cycles).

Transcript identification, quantification, and circadian analysis

The processed sequences were aligned to v3.1 of the Bd21 genome using HISAT2 (Kim *et al.*, 2015)(**Supporting Information Table 1**). This annotation of the genome contains 34,310 protein-coding loci and 52,972 protein-coding transcripts. Read counts were then normalized using DESeq2 (Love *et al.*, 2014). In each time course, approximately 80% of all transcripts were detected, and the distribution of the normalized expression levels were comparable (**Supporting Information Fig. 1**). Unless specified otherwise, all expression quantities reported are at the transcript (as opposed to gene) level, accounting for potential splice variants. After normalization, MetaCycle (Wu *et al.*, 2016a) was used to assess rhythmicity, with cycling genes called using a *p*-value cutoff of 0.01. Phase, period, and amplitude metrics were extracted from MetaCycle output.

Computational analysis

Computational analysis was performed in R (version 3.6.0) using resources from the Massachusetts Green High Performance Computing Center. Venn diagrams were generated using the Limma package (Ritchie *et al.*, 2015). Sinaplots were generated using the ggforce R package (Pedersen, 2019). Remaining plots were created using ggplot2 (Wickham, 2016). Data transformation was accomplished with either the dplyr package (Wickham *et al.*, 2019), or the data.table package (Dowle & Srinivasan, 2019). Coefficient of variance was determined using the raster package (Hijmans, 2019). Tests of statistical significance for period lengths and relative amplitudes were conducted by first performing analysis of variance and then based on the distribution of the data we assessed significance using a pairwise Wilcoxon rank sum test (Haynes, 2013). The transcriptome data were integrated into the Brachypodium eFP browser, (http://bar.utoronto.ca/efp_brachypodium/cgi-bin/efpWeb.cgi) (Winter *et al.*, 2007). The eFP browser enables the visualization of gene expression levels with a pictograph heatmap and the download and visualization of tables and charts for expression values of individual genes. Raw read data were deposited in the European Nucleotide Archive for public access (Accession: PRJEB32498).

Pathway enrichment analysis

NCBI BLAST and Phytozome (Altschul *et al.*, 1990; Goodstein *et al.*, 2011) were used to find orthologs for all *B. distachyon* v3.1 genes as the reciprocal best match to *A. thaliana* TAIRv10 protein sequences. Genes that did not significantly match a corresponding gene in *A. thaliana* were discarded from this analysis. *Arabidopsis thaliana* biological process gene ontology (GO) annotations were obtained from http://ge-lab.org/gskb/. The Java implementation of PSEA1.1 (Zhang *et al.*, 2016) was used for analysis, with 0-28 for the "domain" parameter, and 10 for the "minimum items" parameter. For Kuiper's test, the distribution of GO terms was compared with an empirically-determined background distribution. Gene identifiers were submitted to g:Profiler (Raudvere *et al.*, 2019) for KEGG and Wiki pathway enrichment analysis.

Hierarchical cluster analysis

To find groups of genes with similar expression profiles, we first filtered all transcripts to only include those expressed at least once in all four time courses. Transcript expression was then standardized by computing z-scores within each condition. Standardized transcript expression dissimilarity was assessed using Pearson's correlation and hierarchically clustered according to the complete linkage method of agglomeration. The resulting dendrogram was visually analyzed to determine the ideal number of clusters based on the elbow method. Gene expression was then modeled using the GAM method of smoothing to represent a cluster (Wood, 2004). Period length clustering was performed by first normalizing period values relative to their z-score for transcripts that cycled in all of the four time course conditions. Heatmaps were plotted using Heatmap.2 (Warnes *et al.*, 2019).

Phylogenetic analysis

To identify *B. distachyon* orthologs of *A. thaliana RVE*s, *LWD*s, and *LNK*s, we used a BLAST e-value $\leq$ e-60 as the criterion for quickly identifying the immediate homologs for each clade, and larger e-values to extract less related, but phylogenetically relevant sequences. We identified homologs of each clade using *A. thaliana* TAIR10, *B. distachyon* Phytozome v3.1, *Orya sativa* v7.0_JGI, *Populus trichocarpa*

Phytozome v3.0, *Setaria viridis* Phytozome v1.1, and *Solanum lycopersicum* ITAG v3.10 reference genomes. To reconstruct phylogenetic relationships between orthologs, we first aligned protein sequences using MAFFT, with the G-INS-I model (Katoh *et al.*, 2002) and then used the neighbor-joining method for tree construction with 1000 bootstrap samples. The proteins sequences used are provided in **Supporting Information Table 2**.

Cis-regulatory sequence analysis

Cis-regulatory sequence analysis of cycling transcripts was performed by first grouping transcripts based on phase of gene expression in each time course and then selecting putative regulatory sequence up to 1000 bp upstream of the transcriptional start site. HOMER v4.10 (Heinz *et al.*, 2010) was used to compute enrichment scores for transcription factor binding motifs previously identified using DNA-affinity-purified sequencing (DAP-seq, (O'Malley *et al.*, 2016)) among each group of cycling transcripts. Motif enrichment was calculated against the hypergeometric distribution; the significance threshold was set to $p < 0.05$. Similar motifs were determined using the compareMotifs.pl function of HOMER against the global list of known motifs with the default threshold cutoff of 0.6. ELEMENT analysis was carried out as previously described with modifications (Mockler *et al.*, 2007; Michael *et al.*, 2008b; Filichkin *et al.*, 2011; Wai *et al.*, 2019). Briefly, The *B. distachyon* promoters (500 bp) were parsed using the Bd v3.1 gene models and grouped by peak time of expression into phase bins (0 to 28 hrs).

RESULTS

Widespread diurnal regulation of the *Brachypodium distachyon* transcriptome.

In order to fully explore the rhythmic nature of the *B. distachyon* transcriptome, accession Bd21 seeds were entrained in photocycles and thermocycles for 10 d after germination. Growth conditions were then shifted to one of three conditions: photocycles only (light:dark hot:hot, LDHH), thermocycles only (light:light hot:cold, LLHC), or constant conditions (light:light hot:hot, LLHH). A fourth set of samples remained in photocycles and thermocycles (light:dark hot:cold, LDHC). After 12 h of exposure to their new conditions, the emerging leaves of plants were sampled every 3.5 h for a total of 45.5 h, resulting in a collection of 14 time-resolved samples across four conditions. Transcript abundances were then quantified from each of these samples using RNA-seq.

Expression patterns of cyclically expressed genes can be broadly summarized by three parameters: phase (the time of peak expression), period (the average time between peaks), and amplitude (half of the gene expression difference between peak and trough). For each expressed transcript (47,036), we estimated the periodicity and phase under each condition using MetaCycle, which integrates three distinct methods: ARSER, JTK.Cycle, and Lomb-Scargle algorithms, combined using Fisher's method (Yang & Su, 2010; Hughes *et al.*, 2010; Wu *et al.*, 2016a). Phase and period were then calculated as the circular mean of the estimated time of peak expression, and arithmetic mean of each period estimate. Subsequent analysis was restricted to transcripts with a period that ranged from 21 to 28 h. The bimodal *p*-value distribution was very similar across growth conditions (**Supporting Information Fig. 2**), enabling us to use a fixed *p*-value cutoff ($p < 0.01$) to classify transcripts as cyclic without bias towards any specific condition. Based on this analysis, we observed 16,916 transcripts with rhythmic expression in at least one condition, accounting for nearly 36% of the measured transcriptome. The largest number of cycling transcripts, 10,027 (21.3%), was observed in LDHC (**Figure 1**). The same number of transcripts cycled under photocycles or thermocycles alone (7,391; 15.7%) and the smallest number of rhythmic transcripts was measured under constant conditions (1,699; 3.6%). Among pairs of conditions, LDHC and LLHC conditions were most similar in terms of shared rhythmic transcripts (4,531), while LDHC and LDHH exhibited 30% fewer shared rhythmic transcripts (3,156). We also identified several transcripts that did not cycle under any condition, and might be useful as alternative reference genes for targeted assays ((Hong *et al.*, 2008); **Supporting Information Fig. 3, Supporting Information Table 3-4**). These results suggest that temperature cycles are more dominant in driving diurnal regulation of the transcriptome.

Circadian clock genes

Very few circadian clock genes have been functionally characterized in grasses, and none in *B. distachyon*. Therefore, we assembled a list of core circadian clock transcripts based on our analysis of amino acid sequence similarity to *A. thaliana* and by previously described homology and expression behavior in *B. distachyon* (Higgins et al., 2010; Matos et al., 2014; Calixto et al., 2015)(**Supporting Information Fig. 4-6**). To further verify that the *B. distachyon* clock gene orthologs represent true clock genes, we examined whether transcripts from these loci cycle in our transcriptome data. From this analysis, we observed that all putative clock gene orthologs had at least one rhythmic transcript in at least one of the two-day time courses, with the exception of *BdLWD,* which was starkly arrhythmic

(**Figure 2**, **Supporting Information Table 5**). This observation is consistent with the overall transcriptome behavior where average period was greatest in LLHH.

Gene expression phase is concentrated to late day and night by external cues and to dawn and dusk by the circadian clock to dawn and dusk.

We observed that the majority of all cycling transcripts exhibited an approximately 24 h period. In the presence of any external cue, the vast majority of rhythmic transcripts exhibited a peak expression approximately 8 h after dawn or 8 h after dusk (**Figure 3a**). In contrast to these three conditions, a dramatic shift in expression behavior was observed in the absence of external cues, where the majority of cycling transcripts peaked at dusk with a smaller peak at about 2 h after subjective dawn. This shift in phase could be explained by a lengthening of period observed in constant conditions in contrast to the 24 h period observed under LDHH or LLHC (**Figure 3b**). Transcript expression profiles under LDHC exhibited a double peak shortly before and after 24 h, while in LDHH and LLHC, peak expression occurred after or before dawn, respectively. While constant conditions elicited similar peaks in period distribution, more transcripts exhibited a period of about 27 h suggesting the internal period of Bd21 may be longer than 24 h.

Thermocycles are the dominant cue driving the 24 h period of circadian clock-regulated genes.

To further investigate the relative influence of external cues and the circadian clock on rhythmic gene expression patterns, we analyzed the 306 transcripts found to cycle in all four conditions. As noted before for all rhythmic transcripts, we observed significant effects on period length caused by growth conditions for the 306 core cycling genes. Period length was significantly shorter in LLHC and significantly longer in constant conditions (**Supporting Information Table 6**, **Figure 4a**). While the mean expression values were similar in the presence of external cues, the ranges were not. The interquartile range of the period length distribution was within 1 h of 24 h in LDHC and LLHC, whereas the range was much greater in LDHH and LLHH (**Figure 4a**). We used hierarchical clustering of period length to group the core cycling transcripts into four non-overlapping sets. We observed that a plurality of transcripts (140) maintained an approximate 24 h period under LDHC, LDHH, and LLHC (**Figure 4b**), but exhibited a significantly longer period under LLHH. Forty-seven out of the 306 core cyclic transcripts did not show a significant shift in period between entrained and constant conditions (**Figure 4d**), representing relatively robust rhythmic behavior. Interestingly, 77 transcripts exhibited 24 h periods in LDHC and LLHC, but substantially longer periods in LDHH and LLHH (**Figure 4e**), while far fewer (42) transcripts exhibited a 24 h period in LDHC and LDHH but not in LLHC (**Figure 4c**). These results suggest that temperature may have a stronger influence than light on transcript periodicity.

Thermocycles are the dominant cue determining amplitude and average expression.

Circadian amplitude is the range of expression from the midpoint to the minimum (nadir) and maximum (zenith) for a transcript. Relative amplitude therefore is the ratio between the absolute amplitude and a midline expression for a transcript, allowing for comparison of transcripts with differing expression levels. We observed significant differences in mean relative amplitudes between all four conditions (**Figure 5a, Supporting Information Table 7**). Relative amplitudes of transcripts in LDHC and LLHC conditions were similar (though still statistically distinct, $p < 0.01$ Wilcoxon rank sum test), while cyclic transcripts under LLHH exhibited significantly weaker amplitude ($p < 0.01$). Interestingly, LDHH

conditions elicited significantly greater amplitudes among cycling transcripts. We further interrogated the effect of photo- and thermocycles on the amplitude of cycling transcripts by comparing the distribution of expression values. There was a significant increase in mean expression in constant temperature (LDHH and LLHH, **Figure 5b**). Thus, while LDHH and LLHH conditions have opposing impacts on amplitude, both conditions increased mean expression levels (**Figure 5c**). As with the period and phase, amplitude and expression levels in LDHC and LLHC conditions were most similar. Taken together, our results indicate that rhythmic gene expression is strongly influenced by thermocycles, with thermocycles alone being sufficient to reproduce the expression patterns observed in the presence of both photo- and thermocycles. Absent external cues, our results suggest that negative regulation of transcript expression is relieved, thus dampening the amplitude and increasing overall expression.

Gene expression and phase clustering show pathway functions are uniquely or similarly influenced by external cues.

To determine whether specific physiological functions are impacted by differences in external cues, we used Pearson correlation coefficients to hierarchically cluster all transcripts that were expressed in all four conditions. Nine clusters were defined based on patterns of expression across each of the conditions (**Supporting Information Fig. 7**). While we applied no filters for diurnal or circadian rhythms, the profiles for each cluster suggest that daily rhythms were important determinants for clustering of transcript expression patterns (**Figure 6**). Annotations associated with DNA replication and repair or homologous recombination were significantly enriched for genes in cluster 1, which were rhythmic under photocycles and peaked during the day. Terms associated with ethylene signaling, genetic interaction between sugar and hormone signaling, and non-homologous end-joining involved in DNA repair were enriched among transcripts with daytime expression in the presence of thermocycles (clusters 5 and 8). Our results also suggest that gene connected to biosynthesis of secondary metabolites, carbon fixation, and peroxisome activity are expressed during the night and regulated by both photo- and themrocycles to the same time-of-day (cluster 7). Terms associated with mRNA surveillance, which is involved in the quality control and degradation of mRNA, were enriched in cluster 4, which tended to be expressed during the day under thermocycles, but at night under photocycles. The opposite pattern was observed for spliceosome pathway-associated annotations in cluster 9, where expression peaked during the night in the presence of thermocycles and the day under photocycles alone. Genes annotated as aminoacyl-tRNA biosynthesis components were enriched in cluster 6, with peak expression at dusk under all three entrainment conditions. Other clusters of genes that were minimally affected by external cues were enriched for terms associated with processing and transport of RNA, ribosome biogenesis, photosynthetic antenna proteins, and plant-pathogen interactions (clusters 2 and 3). The trendlines in constant conditions did not show a strong circadian waveform in any of the clusters identified. Consistent with our other observations, clusters of genes with rhythmic expression patterns tended to have expression restricted to dawn or dusk, and were more heavily influenced by thermocycles than photocycles (**Figure 6**).

Transcripts that were rhythmic in at least one time course were grouped by phase and tested for enrichment of biological process gene ontology (GO) terms (**Supporting Information Fig. 8**). This analysis was meant to identify biological processes that are diurnal or circadian clock controlled, and whether they exhibit variable expression depending on diurnal condition. Notably, secondary cell wall

biosynthesis (including terms associated with 'secondary cell wall biogenesis', and 'lignin biosynthetic process') appeared to be thermocycle regulated from this analysis (**Supporting Information Fig. 8, Figure 7**). This observation is also consistent with gene expression profiles exhibited by hierarchical cluster 7 (**Figure 6**) and suggests strong coordinated action of thermocycles in regulating control of plant structural properties to the night. GO terms associated with pathogen defense pathways appeared in both thermocycle (response to fungus, jasmonic acid biosynthetic process, defense response to bacterium) and photocycle (response to chitin, response to jasmonic acid stimulus, defense response) driven conditions independently, but the same terms were not associated with all conditions. This is consistent with our hierarchical clustering observations that found pathogen responses were not strongly driven by any one condition (cluster 3; **Supporting Information Fig. 8**). Similar to our observations from hierarchical clustering of gene expression profiles, GO term enrichment analysis suggests that photocycles elicited rhythmic expression of gene sets related to cellular processes, such as DNA replication, translational elongation, and tricarboxylic acid cycle. These groups tended to be expressed during the day (**Supporting Information Fig. 8**). The only terms to appear across all conditions are response to heat, 'photosynthesis light harvesting', and 'photosynthesis'.

Time-of-day specific *cis*-regulatory sequences.

It has been shown that some *cis*-regulatory sequences controling time-of-day expression are conserved across monocots and dicots (Michael *et al.*, 2008b; Filichkin *et al.*, 2011). Three *cis*-element modules made up of the morning element (ME:CCACAC), evening element (EE:AAATATCT) and the telobox (TBX:AAACCCT) along with their associated elements, including CCA1-binding site (CBS:AAAATCT), G-box (CACGTG), GATA, starch box (SPX:AAGCCC) and protein box (PBX:ATGGGCCG) (Michael *et al.*, 2008b,a; Filichkin *et al.*, 2011). To identify known and novel time-ofday-specific *cis*-elements, we used the ELEMENT program to perform an exaustive promoter search for 3-8 bp sequences. We identified 113, 86, 327 and 11 significantly overrepresented *cis*-elements under LDHC, LLHC, LDHH and LLHH, respectively, including ME, EE, G-box core (ACGT), TBX, PBX and SBX (**Figure 8**) (Michael *et al.*, 2008b). However, the TBX, SBX and PBX elements were only significantly overrepresented in LDHH conditions. Inspection of all significantly overrepresented 3-8 bp sequences revealed a clear pattern that conditions with thermocycles are alike and distinct from those with photocycles alone (**Supporting Information Fig. 9**). These results suggest that thermocycles override the impact of photocycles on gene expression regulation, consistent with our previous results that thermocycles play a distinct and dominant role in coordinating time-of-day expression.

DNA affinity purification sequencing (DAP-seq) is a powerful method to identify transcription factor binding sites *in vitro* (O'Malley *et al.*, 2016). We leveraged DAP-seq binding site motifs from *A. thaliana* to link time-of-day motifs to their putative transcription factors in the *B. distachyon* time courses. We identified 291 (out of 477 total DAP-seq motifs) significantly enriched motifs, including the core diurnal elements EE, GATA, TBX and G-box (**Figure 9**, **Supporting Information Fig. 10)**. In contrast to ELEMENT, This approach enabled us to identify larger, split elements like VNS (VND/NST/SND, CTTNNNNNNAAG, (Olins *et al.*, 2018)), which was enriched in constant conditions and thermocycles, suggesting that it is very likely part of circadian clock regulation. In addition, we observed enrichment for the CACT motif in the morning in LDHC and LDHH. This element is associated with C2H2 family transcription factors (O'Malley *et al.*, 2016), and is thus a potentially photocycle responsive motif (**Supporting Information Fig. 11**). The CRT/DRE motif (CCGAC, (Stockinger *et al.*, 1997; Liu *et al.*, 1998)), which is bound by CBF type AP2-EREBP proteins, is enriched in midday- and nighttime-expressed transcripts. In addition to the

CRT/DRE motif, three other motifs were enriched in the nighttime: C2C2-Dof binding AAAAAGG (Ko *et al.*, 2016), WRKY-binding W-box GTCAA (Ulker & Somssich, 2004), and bZIP binding HEX element TGACGT (Schindler *et al.*, 1992). The C2C2-Dof site and the W-box were enriched in all diurnal conditions but not constant conditions. The bZIP site and CRT/DRE motif were enriched in constant conditions and in the presence of thermocycles.

DISCUSSION

Daily rhythms in transcript abundance are either a direct response to predictable environmental cues including photocycles, thermocycles, and humidity cycles, or they are generated by the circadian clock. Most estimates of daily gene expression patterns have been determined for protein-coding genes using gene or genome tiling microarrays (Edwards *et al.*, 2006; Covington *et al.*, 2008; Michael *et al.*, 2008b; Hazen *et al.*, 2009; Khan *et al.*, 2010; Filichkin *et al.*, 2011). More recently, RNA-seq was applied to measure diurnal or circadian-associated transcript expression in sugarcane, *S. viridis*, *Sedum album*, lettuce, and Douglas fir (Hotta *et al.*, 2013; Higashi *et al.*, 2016; Cronn *et al.*, 2017; Huang *et al.*, 2017; Wai *et al.*, 2019). Estimates for the proportion of protein-coding genes that are controlled by the circadian clock generally range between 6 and 15%. Species with values well outside this range include *S. viridis* with 1.2% when entrained in thermocycles alone and 33% in sugarcane (Hotta *et al.*, 2013; Huang *et al.*, 2017). Here we report that 3.6% of all *B. distachyon* transcripts are regulated by the circadian clock, which is small relative to other species. It is worth noting that different analyses applied to the same dataset can identify different rhythmic gene sets (Khan *et al.*, 2010; Hotta *et al.*, 2013; Hughes *et al.*, 2017), potentially due to differences in entrainment conditions, as well as other environmental parameters including light intensity and temperature range. Thus, comparisons of the proportion of circadian-clock-regulated genes among species should be made cautiously, with consideration of the method used to measure and analyze transcript abundance and entrainment conditions. Keeping these limitations in mind, we observed a comparable number of rhythmic genes in the presence of external cues and a relatively low number in constant conditions between *B. distachyon* and other species. This observation suggests that the circadian clock has a relatively minor role in *B. distachyon* gene regulation.

In the presence of external cues, peak gene expression was concentrated at the end of the day and night. In constant conditions there was a dramatically different pattern, with dusk as the most represented phase, followed by subjective dawn. A concentration of genes that peak in expression at the end of the day or at night in some combination of photo- and thermocycles was similarly observed in *A. thaliana*, poplar, rice, and Douglas fir (Covington *et al.*, 2008; Michael *et al.*, 2008b; Filichkin *et al.*, 2011; Cronn *et al.*, 2017);(Michael *et al.*, 2008b; Hazen *et al.*, 2009). In maize and sugarcane, the most abundant phases were centered around dawn and dusk (Khan *et al.*, 2010; Hotta *et al.*, 2013), similar to the phase expression profile in this study. However, only constant conditions were reported for maize (Khan *et al.*, 2010) and sugarcane (Hotta *et al.*, 2013) and not similarly described for rice (Filichkin *et al.*, 2011). In barley and rice, the expression of putative clock genes was measured under entrainment and constant conditions with no change in period or phase noted between conditions (Murakami *et al.*, 2007; Filichkin *et al.*, 2011; Campoli *et al.*, 2012). Thus, a similar phase shift was neither tested nor observed in several grass species.

The change in phase we observed may be a result of the striking period difference observed in constant conditions. Our analysis was restricted to genes with periods ranging from 21 to 28 h. A vast majority of rhythmic transcripts cycled with a period between 23 and 25 h. While some genes cycled with a similar period in constant conditions, the most abundant period for genes in constant conditions was much longer, with a range between 26 to 28 h. A meta-analysis of 11 different *A. thaliana* time courses did not

report a lengthening of period in constant conditions for the Col-0 accession (Michael *et al.*, 2008b). Similarly, *S. viridis* genes that were rhythmic under constant conditions exhibited an approximate 24 h period. In contrast, variation in period length has been measured in a number of other species, and in many cases mutations conferring clock-related phenotypes in crop plants have been identified (Bendix *et al.*, 2015; Greenham *et al.*, 2017)(Michael *et al.*, 2003; Dodd *et al.*, 2005; Srivastava *et al.*, 2019). Also, light intensity is known to influence period length, and has been shown to result in changes at very low fluences (Somers *et al.*, 1998; Oakenfull & Davis, 2017). Thus, we cannot rule out an effect of genetic variation or light intensity in our data set without further testing. The 27 h period length estimation in constant conditions in *B. distachyon* may reflect the specific period of the accession tested, but within the range of natural genetic variation observed in several species.

A number of factors are known to alter amplitudes of gene expression. Cold dampens amplitude in *A. thaliana* and a local infection of the bacterial pathogen *Pseudomonas syringae* as well as salicylic acid or H_2O_2 results in a systematic decrease in amplitude (Bieniawska *et al.*, 2008; Li *et al.*, 2018). Several *A. thaliana* circadian clock mutants exhibit a decrease in amplitude up to a total loss of circadian function (Nagel & Kay, 2013). Often, these changes in amplitude cause an increase in average gene expression because the nadir is not as low. Our results suggest that a self sustaining circadian clock provides only a small portion of the daily repression that results in robust amplitude and waveform.

Circadian clock genes and their expression behavior are largely conserved between grasses and eudicots (McClung, 2010; Campoli *et al.*, 2012)(Mockler *et al.*, 2007; Michael *et al.*, 2008b; Filichkin *et al.*, 2011; Wai *et al.*, 2019)). Several genes, namely *BdRVE86*, *BdLNK1*, *BdCHE*, *BdPRR73*, *BdELF4-likeA*, and *BdELF3* were not detected as significantly circadian clock regulated in this study. Under entrainment conditions, the average clock gene cycled with a nearly 24 h period, but this period lengthened to greater than 26 h in constant conditions. It may be that the absence of rhythmic expression of one or more circadian clock genes resulted in a substantially slower circadian clock in *B. distachyon*. Mutations in all of the arrhythmic genes can result in a long period or arrhythmic expression in *A. thaliana* (Nagel & Kay, 2013). ELF3 is a particularly interesting candidate as naturally occurring allelic variants in *A. thaliana* are linked to poor rhythms (Box *et al.*, 2015).

Analysis of the *cis*-regulatory regions of rhythmic genes with similar time-of-day expression identified sequence motifs that are candidates for functional determinants of that expression behavior. In spite of the relatively small number of circadian-clock-regulated transcripts identified in our study, we recovered a robust signature for the evening element under all four conditions. The G-box, a morning-enriched motif in other systems (Zdepski *et al.*, 2008; Filichkin *et al.*, 2011), was enriched in both morning and evening expressed genes in thermocycles and constant conditions. We also observed enrichment of the CBF binding site among evening-phased genes in all conditions except LDHH. The CBF family of transcription factors is strongly associated with the circadian clock, providing temperature input by directly binding the *LUX* promoter (Chow *et al.*, 2014; Gierczik *et al.*, 2017). Neither the G-box nor the CRT element was overrepresented under photocycles alone. We also observed enrichment of the CACT motif among genes with early morning peak expression under thermocycles and constant conditions. The CACT motif is a binding target for several members of the C2H2 family of transcription factors

(O'Malley *et al.*, 2016), and has not been shown to be rhythmically overrepresented as a standalone motif; however, Hudson and Quail (2003) did show that a CACT motif, attached to an AC-element or morning element, is a potentially novel circadian-regulated binding motif. The CACT motif has also been shown to be contained in a larger motif (CAGCCACTA) conserved in promoter regions of LHY orthologs (Spensley *et al.*, 2009). We further identified several motifs not previously described as having a role in diurnal gene expression or circadian clock output from time course analysis. These include the VNS, W-box, and Dof binding motif. The VNS motif featured heavily in secondary cell wall development, and is a consensus sequence bound by the VND, NST, and SND NAC transcription factors (Olins *et al.*, 2018). Consistent with our observation of rhythmic secondary cell wall genes, this motif was enriched in both diurnal and constant conditions. The W-box is a binding target for some WRKY transcription factors, which have been shown to interact with the circadian clock to help regulate senescence (Kim *et al.*, 2018). ChIP-seq experiments have revealed the Dof-binding motif, AAAAAGG, to be a target of ZmCCA1 and LHY (Ko *et al.*, 2016)(Adams *et al.*, 2018). Similarly, several CDF transcription factors are clock regulated and play a crucial role in photoperiodic timing (Goralogia *et al.*, 2017). The HEX motif is associated with bZIP-binding in plants and represent a possible source of entrainment for the circadian clock through metabolic adjustments in response to sugar availability (Schindler *et al.*, 1992(Frank *et al.*, 2018).

Rhythmic growth in plants has been observed across numerous species, and depends on both internal and external cues (Walter *et al.*, 2009; Farre, 2012). In *A. thaliana*, the rate of hypocotyl elongation is greatest at the end of the night and is heavily influenced by photoreceptors and the circadian clock (Dowson-Day & Millar, 1999; Nozue *et al.*, 2007). In grasses, temperature is the dominant cue that determines the relative rate of cell division and elongation (Watts, 1971; Poiré *et al.*, 2010). Previously, we reported that the rate of *B. distachyon* leaf elongation was regulated by thermocycles (Matos *et al.*, 2014). Here we observed that genes associated with secondary cell wall biosynthesis, including *CELLULOSE SYNTHASE A4/7/8* and several lignin pathway genes (Coomey & Hazen, 2016), were regulated by thermocycles with peak expression occurring at night. Rhythmic coexpression of lignin and cell-wall-related genes has been observed in maize and *A. thaliana*, but often with different timing or following different cues (Michael *et al.*, 2008a; Khan *et al.*, 2010). Indeed, in *A. thaliana*, carbon status and light influence lignin gene expression and hypocotyl lignification (Rogers *et al.*, 2005). It is interesting to note that our gene expression results clearly show that expression of secondary-wall-related genes follows thermocycles, but is antiphasic to reported maximal elongation rates. This suggests that rhythmic elongation under warm temperatures may be followed by rhythmic wall thickening under nighttime temperatures.

In summary, both internal and external cues caused pervasive circadian rhythms in *B. distachyon*. The total effect on rhythmic gene expression was similar between photo- and thermocycles, and more than 21% of genes had rhythmic expression in the presence of both cues. Thermocycling appears to be the prevailing signal. The overlap was greatest between genes that commonly cycled in LDHC and LLHC. Rhythmic gene expression under thermocycles had a more narrow distribution and a period closer to 24 h for genes rhythmic in all four conditions. Overall expression level and relative amplitude was most similar between LDHC and LLHC. Hierarchical clustering revealed pathway enriched groups of genes more commonly expressed between LDHC and LLHC and clustering of gene sets based on phase of expression revealed distinctly synchronized pathways between thermocycles and photocycles. The

relative importance of thermocycles is consistent with the observation that grasses are uniquely void of elongation growth rhythms in constant conditions or in the presence of photocycles alone (Poiré *et al.*, 2010; Matos *et al.*, 2014).

AUTHOR CONTRIBUTIONS

BC, SH, and SK conceived and designed the study. BC, MR, and TD acquired the data. KM, BC, CY, JC, NH, TM, and SH analyzed and interpreted the data. KM, BC, JC, TM, and SH drafted the manuscript.

FUNDING

This work was supported by Office of Science, Biological and Environmental Research, Department of Energy [DE-FG02-08ER64700DE and DE-SC0006621 to S.P.H. and S.A.K.] and The National Science Foundation Division of Integrative Organismal Systems [NSF IOS-1558072 to S.P.H.]

REFERENCES

Adams S, Grundy J, Veflingstad SR, Dyer NP, Hannah MA, Ott S, Carré IA. **2018**. Circadian control of abscisic acid biosynthesis and signalling pathways revealed by genome-wide analysis of LHY binding targets. *New Phytologist* **220**: 893–907.

Altschul SF, Gish W, Miller W, Myers EW, Lipman DJ. **1990**. Basic local alignment search tool. *Journal of Molecular Biology* **215**: 403–410.

Arsovski AA, Pradinuk J, Guo XQ, Wang S, Adams KL. **2015**. Evolution of cis-regulatory elements and regulatory networks in duplicated genes of Arabidopsis. *Plant Physiology* **169**: 2982.

Bendix C, Marshall CM, Harmon FG. **2015**. Circadian Clock Genes Universally Control Key Agricultural Traits. *Molecular Plant* **8**: 1135–1152.

Bieniawska Z, Espinoza C, Schlereth A, Sulpice R, Hincha DK, Hannah MA. **2008**. Disruption of the Arabidopsis circadian clock is responsible for extensive variation in the cold-responsive transcriptome. *Plant Physiology* **147**: 263–279.

Box MS, Huang BE, Domijan M, Jaeger KE, Khattak AK, Yoo SJ, Sedivy EL, Jones DM, Hearn TJ, Webb AAR, *et al.* 2015. ELF3 controls thermoresponsive growth in Arabidopsis. *Current Biology: CB* **25**: 194–199.

Calixto CPG, Waugh R, Brown JWS. **2015**. Evolutionary relationships among barley and Arabidopsis core circadian clock and clock-associated genes. *Journal of Molecular Evolution* **80**: 108–119.

Campoli C, Shtaya M, Davis S, von Korff M. **2012**. Expression conservation within the circadian clock of a monocot: natural variation at barley *Ppd-H1* affects circadian expression of flowering time genes, but

not clock orthologs. *BMC Plant Biology* **12**: 97.

Casal JJ, Qüesta JI. **2018**. Light and temperature cues: multitasking receptors and transcriptional integrators. *The New Phytologist* **217**: 1029–1034.

Choudhary MK, Nomura Y, Wang L, Nakagami H, Somers DE. **2015**. Quantitative Circadian Phosphoproteomic Analysis of Arabidopsis Reveals Extensive Clock Control of Key Components in Physiological, Metabolic, and Signaling Pathways. *Molecular & Cellular Proteomics: MCP* **14**: 2243–2260.

Chow BY, Sanchez SE, Breton G, Pruneda-Paz JL, Krogan NT, Kay SA. **2014**. Transcriptional regulation of LUX by CBF1 mediates cold input to the circadian clock in Arabidopsis. *Current Biology: CB* **24**: 1518–1524.

Coomey JH, Hazen SP. **2016**. Brachypodium distachyon as a Model Species to Understand Grass Cell Walls. In: Vogel JP, ed. Genetics and Genomics of Brachypodium. Cham: Springer International Publishing, 197–217.

Covington M, Maloof J, Straume M, Kay S, Harmer S. **2008**. Global transcriptome analysis reveals circadian regulation of key pathways in plant growth and development. *Genome Biology* **9**: R130.

Cronn R, Dolan PC, Jogdeo S, Wegrzyn JL, Neale DB, St Clair JB, Denver DR. **2017**. Transcription through the eye of a needle: daily and annual cyclic gene expression variation in Douglas-fir needles. *BMC Genomics* **18**: 558.

Dodd AN, Salathia N, Hall A, Kevei E, Toth R, Nagy F, Hibberd JM, Millar AJ, Webb AA. **2005**. Plant circadian clocks increase photosynthesis, growth, survival, and competitive advantage. *Science* **309**: 630–633.

Dowle M, Srinivasan A. **2019**. data.table: Extension of `data.frame`.

Dowson-Day MJ, Millar AJ. **1999**. Circadian dysfunction causes aberrant hypocotyl elongation patterns in Arabidopsis. *The Plant Journal: for cell and molecular biology* **17**: 63–71.

Edwards KD, Anderson PE, Hall A, Salathia NS, Locke JC, Lynn JR, Straume M, Smith JQ, Millar AJ. **2006**. FLOWERING LOCUS C mediates natural variation in the high-temperature response of the Arabidopsis circadian clock. *The Plant Cell* **18**: 639–650.

Farinas B, Mas P. **2011**. Functional implication of the MYB transcription factor RVE8/LCL5 in the circadian control of histone acetylation. *The Plant Journal: for cell and molecular biology* **66**: 318–329.

Farre EM. **2012**. The regulation of plant growth by the circadian clock. *Plant Biology* **14**: 401–410.

Farré EM, Harmer SL, Harmon FG, Yanovsky MJ, Kay SA. **2005**. Overlapping and distinct roles of PRR7 and PRR9 in the Arabidopsis circadian clock. *Current Biology: CB* **15**: 47–54.

Filichkin SA, Breton G, Priest HD, Dharmawardhana P, Jaiswal P, Fox SE, Michael TP, Chory J, Kay SA, Mockler TC. **2011**. Global profiling of rice and poplar transcriptomes highlights key conserved circadian-controlled cathways and *cis*-regulatory modules. *PloS One* **6**: e16907.

Franklin KA, Toledo-Ortiz G, Pyott DE, Halliday KJ. **2014**. Interaction of light and temperature signalling.

Journal of Experimental Botany **65**: 2859–2871.

Frank A, Matiolli CC, Viana AJC, Hearn TJ, Kusakina J, Belbin FE, Wells Newman D, Yochikawa A, Cano-Ramirez DL, Chembath A, *et al.* 2018. Circadian Entrainment in Arabidopsis by the Sugar-Responsive Transcription Factor bZIP63. *Current Biology: CB* **28**: 2597–2606.e6.

Gendron JM, Pruneda-Paz JL, Doherty CJ, Gross AM, Kang SE, Kay SA. **2012**. Arabidopsis circadian clock protein, TOC1, is a DNA-binding transcription factor. *Proceedings of the National Academy of Sciences of the United States of America* **109**: 3167–3172.

Gierczik K, Novák A, Ahres M, Székely A, Soltész A, Boldizsár Á, Gulyás Z, Kalapos B, Monostori I, Kozma-Bognár L, *et al.* 2017. Circadian and Light Regulated Expression of CBFs and their Upstream Signalling Genes in Barley. *International Journal of Molecular Sciences* **18**.

Gil K-E, Kim W-Y, Lee H-J, Faisal M, Saquib Q, Alatar AA, Park C-M. **2017**. ZEITLUPE Contributes to a Thermoresponsive Protein Quality Control System in Arabidopsis. *The Plant Cell* **29**: 2882–2894.

Goodstein DM, Shu S, Howson R, Neupane R, Hayes RD, Fazo J, Mitros T, Dirks W, Hellsten U, Putnam N, *et al.* 2011. Phytozome: a comparative platform for green plant genomics. *Nucleic Acids Research* **40**: D1178–D1186.

Goralogia GS, Liu T-K, Zhao L, Panipinto PM, Groover ED, Bains YS, Imaizumi T. **2017**. CYCLING DOF FACTOR 1 represses transcription through the TOPLESS co-repressor to control photoperiodic flowering in Arabidopsis. *The Plant Journal: for cell and molecular biology* **92**: 244–262.

Greenham K, Lou P, Puzey JR, Kumar G, Arnevik C, Farid H, Willis JH, McClung CR. **2017**. Geographic Variation of Plant Circadian Clock Function in Natural and Agricultural Settings. *Journal of Biological Rhythms* **32**: 26–34.

Green RM, Tingay S, Wang Z-Y, Tobin EM. **2002**. Circadian rhythms confer a higher level of fitness to Arabidopsis plants. *Plant Physiology* **129**: 576–584.

Handakumbura PP, Brow K, Whitney IP, Zhao K, Sanguinet KA, Lee SJ, Olins J, Romero-Gamboa SP, Harrington MJ, Bascom CJ, *et al.* 2018. *SECONDARY WALL ASSOCIATED MYB1* is a positive regulator of secondary cell wall thickening in *Brachypodium distachyon* and is not found in the Brassicaceae. *The Plant Journal: for cell and molecular biology* **0**.

Harmer SL, Hogenesch JB, Straume M, Chang HS, Han B, Zhu T, Wang X, Kreps JA, Kay SA. **2000**. Orchestrated transcription of key pathways in Arabidopsis by the circadian clock. *Science* **290**: 2110–2113.

Haynes W. **2013**. Wilcoxon Rank Sum Test. In: Dubitzky W, Wolkenhauer O, Cho K-H, Yokota H, eds. Encyclopedia of Systems Biology. New York, NY: Springer New York, 2354–2355.

Hazen SP, Naef F, Quisel T, Gendron JM, Chen H, Ecker JR, Borevitz JO, Kay SA. **2009**. Exploring the transcriptional landscape of plant circadian rhythms using genome tiling arrays. *Genome Biology* **10**: R17.

Heinz S, Benner C, Spann N, Bertolino E, Lin YC, Laslo P, Cheng JX, Murre C, Singh H, Glass CK. **2010**. Simple combinations of lineage-determining transcription factors prime *cis*-regulatory elements

required for macrophage and B cell identities. *Molecular Cell* **38**: 576–589.

Higashi T, Aoki K, Nagano AJ, Honjo MN, Fukuda H. **2016**. Circadian Oscillation of the Lettuce Transcriptome under Constant Light and Light-Dark Conditions. *Frontiers in Plant Science* **7**: 1114.

Higgins JA, Bailey PC, Laurie DA. **2010**. Comparative genomics of flowering time pathways using *Brachypodium distachyon* as a model for the temperate grasses. *PloS One* **5**: e10065.

Hijmans RJ. **2019**. raster: Geographic Data Analysis and Modeling.

Hong S-Y, Seo P, Yang M-S, Xiang F, Park C-M. **2008**. Exploring valid reference genes for gene expression studies in Brachypodium distachyon by real-time PCR. *BMC Plant Biology* **8**: 112.

Hotta CT, Nishiyama MY Jr, Souza GM. **2013**. Circadian rhythms of sense and antisense transcription in sugarcane, a highly polyploid crop. *PloS One* **8**: e71847.

Hsu PY, Devisetty UK, Harmer SL. **2013**. Accurate timekeeping is controlled by a cycling activator in Arabidopsis. *eLife* **2**: e00473.

Huang H, Gehan MA, Huss SE, Alvarez S, Lizarraga C, Gruebbling EL, Gierer J, Naldrett MJ, Bindbeutel RK, Evans BS, Mockler TC, Nusinow DA. 2017. Cross-species complementation reveals conserved functions for EARLY FLOWERING 3 between monocots and dicots. *Plant Direct* **1**: e00018.

Huang W, Pérez-García P, Pokhilko A, Millar AJ, Antoshechkin I, Riechmann JL, Mas P. **2012**. Mapping the core of the Arabidopsis circadian clock defines the network structure of the oscillator. *Science* **336**: 75–79.

Hudson ME, Quail PH. **2003**. Identification of promoter motifs involved in the network of phytochrome A-regulated gene expression by combined analysis of genomic sequence and microarray data. *Plant Physiology* **133**: 1605–1616.

Hughes ME, Abruzzi KC, Allada R, Anafi R, Arpat AB, Asher G, Baldi P, de Bekker C, Bell-Pedersen D, Blau J, *et al.* 2017. Guidelines for Genome-Scale Analysis of Biological Rhythms. *Journal of Biological Rhythms* **32**: 380–393.

Hughes ME, Hogenesch JB, Kornacker K. **2010**. JTK_CYCLE: an efficient nonparametric algorithm for detecting rhythmic components in genome-scale data sets. *Journal of Biological Rhythms* **25**: 372–380.

James AB, Syed NH, Bordage S, Marshall J, Nimmo GA, Jenkins GI, Herzyk P, Brown JWS, Nimmo HG. **2012**. Alternative splicing mediates responses of the Arabidopsis circadian clock to temperature changes. *The Plant Cell* **24**: 961–981.

Jung J-H, Domijan M, Klose C, Biswas S, Ezer D, Gao M, Khattak AK, Box MS, Charoensawan V, Cortijo S, *et al.* 2016. Phytochromes function as thermosensors in Arabidopsis. *Science* **354**: 886–889.

Kamioka M, Takao S, Suzuki T, Taki K, Higashiyama T, Kinoshita T, Nakamichi N. **2016**. Direct Repression of Evening Genes by CIRCADIAN CLOCK-ASSOCIATED1 in the Arabidopsis Circadian Clock. *The Plant Cell* **28**: 696–711.

Katoh K, Misawa K, Kuma K, Miyata T. **2002**. MAFFT: a novel method for rapid multiple sequence

alignment based on fast Fourier transform. *Nucleic Acids Research* **30**: 3059–3066.

Khan S, Rowe SC, Harmon FG. **2010**. Coordination of the maize transcriptome by a conserved circadian clock. *BMC Plant Biology* **10**: 126.

Kim H, Kim HJ, Vu QT, Jung S, McClung CR, Hong S, Nam HG. **2018**. Circadian control of ORE1 by PRR9 positively regulates leaf senescence in Arabidopsis. *Proceedings of the National Academy of Sciences of the United States of America* **115**: 8448–8453.

Kim D, Langmead B, Salzberg SL. **2015**. HISAT: a fast spliced aligner with low memory requirements. *Nature Methods* **12**: 357.

Kolmos E, Herrero E, Bujdoso N, Millar AJ, Tóth R, Gyula P, Nagy F, Davis SJ. **2011**. A reduced-function allele reveals that EARLY FLOWERING3 repressive action on the circadian clock is modulated by phytochrome signals in Arabidopsis. *The Plant Cell* **23**: 3230–3246.

Ko DK, Rohozinski D, Song Q, Taylor SH, Juenger TE, Harmon FG, Chen ZJ. **2016**. Temporal Shift of Circadian-Mediated Gene Expression and Carbon Fixation Contributes to Biomass Heterosis in Maize Hybrids. *PLoS Genetics* **12**: e1006197.

Kumar SV, Wigge PA. **2010**. H2A.Z-containing nucleosomes mediate the thermosensory response in Arabidopsis. *Cell* **140**: 136–147.

Lee C-M, Feke A, Li M-W, Adamchek C, Webb K, Pruneda-Paz J, Bennett EJ, Kay SA, Gendron JM. **2018**. Decoys Untangle Complicated Redundancy and Reveal Targets of Circadian Clock F-Box Proteins. *Plant Physiology* **177**: 1170–1186.

Lee C-M, Thomashow MF. **2012**. Photoperiodic regulation of the C-repeat binding factor (CBF) cold acclimation pathway and freezing tolerance in Arabidopsis thaliana. *Proceedings of the National Academy of Sciences of the United States of America* **109**: 15054–15059.

Legris M, Klose C, Burgie ES, Rojas CCR, Neme M, Hiltbrunner A, Wigge PA, Schäfer E, Vierstra RD, Casal JJ. **2016**. Phytochrome B integrates light and temperature signals in Arabidopsis. *Science* **354**: 897–900.

Li Z, Bonaldi K, Uribe F, Pruneda-Paz JL. **2018**. A Localized Pseudomonas syringae Infection Triggers Systemic Clock Responses in Arabidopsis. *Current biology: CB* **28**: 630–639.e4.

Li G, Siddiqui H, Teng Y, Lin R, Wan X-Y, Li J, Lau O-S, Ouyang X, Dai M, Wan J, *et al.* 2011. Coordinated transcriptional regulation underlying the circadian clock in Arabidopsis. *Nature Cell Biology* **13**: 616–622.

Liu XL, Covington MF, Fankhauser C, Chory J, Ry Wagner D. **2001**. ELF3 Encodes a Circadian Clock–Regulated Nuclear Protein That Functions in an Arabidopsis PHYB Signal Transduction Pathway. *The Plant Cell* **13**: 1293–1304.

Liu Q, Kasuga M, Sakuma Y, Abe H, Miura S. **1998**. Two transcription factors, DREB1 and DREB2, with an EREBP/AP2 DNA binding domain separate two cellular signal transduction pathways in drought-and low-temperature-responsive gene expression, respectively, in Arabidopsis. *The Plant Cell* **10:** 1391-1406.

Liu TL, Newton L, Liu M-J, Shiu S-H, Farré EM. **2016**. A G-box-like motif Is necessary for transcriptional

regulation by circadian pseudo-response regulators in Arabidopsis. *Plant Physiology* **170**: 528–539.

Love MI, Huber W, Anders S. **2014**. Moderated estimation of fold change and dispersion for RNA-seq data with DESeq2. *Genome Biology* **15**: 550.

Marshall CM, Tartaglio V, Duarte M, Harmon FG. **2016**. The Arabidopsis sickle Mutant Exhibits Altered Circadian Clock Responses to Cool Temperatures and Temperature-Dependent Alternative Splicing. *The Plant Cell* **28**: 2560–2575.

Más P, Kim W-Y, Somers DE, Kay SA. **2003**. Targeted degradation of TOC1 by ZTL modulates circadian function in Arabidopsis thaliana. *Nature* **426**: 567–570.

Matos DA, Cole BJ, Whitney IP, MacKinnon KJ-M, Kay SA, Hazen SP. **2014**. Daily Changes in Temperature, Not the Circadian Clock, Regulate Growth Rate in Brachypodium distachyon. *PloS One* **9**: e100072.

McClung CR. **2010**. A modern circadian clock in the common angiosperm ancestor of monocots and eudicots. *BMC Biology* **8**: 55.

Michael TP, Breton G, Hazen SP, Priest H, Mockler TC, Kay SA, Chory J. **2008a**. A morning-specific phytohormone gene expression program underlying rhythmic plant growth. *PLoS Biology* **6**: e225.

Michael TP, Mockler TC, Breton G, McEntee C, Byer A, Trout JD, Hazen SP, Shen R, Priest HD, Sullivan CM, *et al.* 2008b. Network discovery pipeline elucidates conserved time-of-day-specific cis-regulatory modules. *PLoS Genetics* **4**: e14.

Michael TP, Salome PA, Yu HJ, Spencer TR, Sharp EL, McPeek MA, Alonso JM, Ecker JR, McClung CR. **2003**. Enhanced fitness conferred by naturally occurring variation in the circadian clock. *Science* **302**: 1049–1053.

Mizuno T, Nomoto Y, Oka H, Kitayama M, Takeuchi A, Tsubouchi M, Yamashino T. **2014**. Ambient temperature signal feeds into the circadian clock transcriptional circuitry through the EC night-time repressor in Arabidopsis thaliana. *Plant & Cell Physiology* **55**: 958–976.

Mockler TC, Michael TP, Priest HD, Shen R, Sullivan CM, Givan SA, McEntee C, Kay SA, Chory J. **2007**. The DIURNAL project: DIURNAL and circadian expression profiling, model-based pattern matching, and promoter analysis. *Cold Spring Harbor symposia on quantitative biology* **72**: 353–363.

Müller LM, Gol L, Jeon J-S, Weber APM, Davis SJ, von Korff M. **2018**. Temperature but not the circadian clock determines nocturnal carbohydrate availability for growth in cereals. *bioRxiv*: 363218.

Murakami M, Tago Y, Yamashino T, Mizuno T. **2007**. Comparative overviews of clock-associated genes of *Arabidopsis thaliana* and *Oryza sativa*. *Plant & Cell Physiology* **48**: 110–121.

Nagel DH, Doherty CJ, Pruneda-Paz JL, Schmitz RJ, Ecker JR, Kay SA. **2015**. Genome-wide identification of CCA1 targets uncovers an expanded clock network in Arabidopsis. *Proceedings of the National Academy of Sciences of the United States of America* **112**: E4802–10.

Nagel DH, Kay SA. **2013**. Complexity in the Wiring and Regulation of Plant Circadian Networks. *Current Biology* **23**: 95–96.

Nieto C, López-Salmerón V, Davière J-M, Prat S. **2015**. ELF3-PIF4 interaction regulates plant growth independently of the Evening Complex. *Current Biology: CB* **25**: 187–193.

Nohales MA, Kay SA. **2016**. Molecular mechanisms at the core of the plant circadian oscillator. *Nature Structural & Molecular Biology* **23**: 1061–1069.

Nohales MA, Liu W, Duffy T, Nozue K, Sawa M, Pruneda-Paz JL, Maloof JN, Jacobsen SE, Kay SA. **2019**. Multi-level Modulation of Light Signaling by GIGANTEA Regulates Both the Output and Pace of the Circadian Clock. *Developmental Cell* **49**: 840–851.e8.

Nozue K, Covington MF, Duek PD, Lorrain S, Fankhauser C, Harmer SL, Maloof JN. **2007**. Rhythmic growth explained by coincidence between internal and external cues. *Nature* **448**: 358–361.

Nusinow DA, Helfer A, Hamilton EE, King JJ, Imaizumi T, Schultz TF, Farre EM, Kay SA. **2011**. The ELF4-ELF3-LUX complex links the circadian clock to diurnal control of hypocotyl growth. *Nature* **475**: 398–402.

Oakenfull RJ, Davis SJ. **2017**. Shining a light on the Arabidopsis circadian clock. *Plant, Cell & Environment* **40**: 2571–2585.

Olins JR, Lin L, Lee SJ, Trabucco GM, MacKinnon KJM, Hazen SP. **2018**. Secondary wall regulating NACs differentially bind at the promoter at a *CELLULOSE SYNTHASE A4* cis-eQTL. *Frontiers in Plant Science* **9**: 1895.

O'Malley RC, Huang S-SC, Song L, Lewsey MG, Bartlett A, Nery JR, Galli M, Gallavotti A, Ecker JR. **2016**. Cistrome and Epicistrome Features Shape the Regulatory DNA Landscape. *Cell* **165**: 1280–1292.

Pedersen TL. **2019**. ggforce: Accelerating 'ggplot2'.

Poiré R, Wiese-Klinkenberg A, Parent B, Mielewczik M, Schurr U, Tardieu F, Walter A. **2010**. Diel time-courses of leaf growth in monocot and dicot species: endogenous rhythms and temperature effects. *Journal of Experimental Botany* **61**: 1751–1759.

Pokhilko A, Fernández AP, Edwards KD, Southern MM, Halliday KJ, Millar AJ. **2012**. The clock gene circuit in Arabidopsis includes a repressilator with additional feedback loops. *Molecular Systems Biology* **8**: 574.

Portolés S, Más P. **2010**. The functional interplay between protein kinase CK2 and CCA1 transcriptional activity is essential for clock temperature compensation in Arabidopsis. *PLoS Genetics* **6**: e1001201.

Raudvere U, Kolberg L, Kuzmin I, Arak T, Adler P, Peterson H, Vilo J. **2019**. g:Profiler: a web server for functional enrichment analysis and conversions of gene lists. *Nucleic Acids Research*.

Rawat R, Takahashi N, Hsu PY, Jones MA, Schwartz J, Salemi MR, Phinney BS, Harmer SL. **2011**. REVEILLE8 and PSEUDO-REPONSE REGULATOR5 form a negative feedback loop within the Arabidopsis circadian clock. *PLoS Genetics* **7**: e1001350.

Reed JW, Nagpal P, Bastow RM, Solomon KS, Dowson-Day MJ, Elumalai RP, Millar AJ. **2000**. Independent Action of ELF3 and phyB to Control Hypocotyl Elongation and Flowering Time. *Plant Physiology* **122**: 1149–1160.

Ritchie ME, Phipson B, Wu D, Hu Y, Law CW, Shi W, Smyth GK. **2015**. limma powers differential expression analyses for RNA-sequencing and microarray studies. *Nucleic Acids Research* **43**: e47.

Rogers LA, Dubos C, Cullis IF, Surman C, Poole M, Willment J, Mansfield SD, Campbell MM. **2005**. Light, the circadian clock, and sugar perception in the control of lignin biosynthesis. *Journal of Experimental Botany* **56**: 1651–1663.

Rugnone ML, Faigón Soverna A, Sanchez SE, Schlaen RG, Hernando CE, Seymour DK, Mancini E, Chernomoretz A, Weigel D, Más P, *et al.* 2013. LNK genes integrate light and clock signaling networks at the core of the Arabidopsis oscillator. *Proceedings of the National Academy of Sciences of the United States of America* **110**: 12120–12125.

Schindler U, Beckmann H, Cashmore AR. **1992**. TGA1 and G-box binding factors: two distinct classes of Arabidopsis leucine zipper proteins compete for the G-box-like element TGACGTGG. *The Plant Cell* **4**: 1309–1319.

Seo PJ, Park M-J, Lim M-H, Kim S-G, Lee M, Baldwin IT, Park C-M. **2012**. A self-regulatory circuit of CIRCADIAN CLOCK-ASSOCIATED1 underlies the circadian clock regulation of temperature responses in Arabidopsis. *The Plant Cell* **24**: 2427–2442.

Sibout R, Proost S, Hansen BO, Vaid N, Giorgi FM, Ho-Yue-Kuang S, Legée F, Cézart L, Bouchabké-Coussa O, Soulhat C, *et al.* 2017. Expression atlas and comparative coexpression network analyses reveal important genes involved in the formation of lignified cell wall in Brachypodium distachyon. *The New Phytologist* **215**: 1009–1025.

Somers DE, Devlin PF, Kay SA. **1998**. Phytochromes and cryptochromes in the entrainment of the Arabidopsis circadian clock. *Science* **282**: 1488–1490.

Spensley M, Kim J-Y, Picot E, Reid J, Ott S, Helliwell C, Carré IA. **2009**. Evolutionarily conserved regulatory motifs in the promoter of the Arabidopsis clock gene LATE ELONGATED HYPOCOTYL. *The Plant Cell* **21**: 2606–2623.

Srivastava D, Shamim, Kumar M, Mishra A, Maurya R, Sharma D, Pandey P, Singh KN. **2019**. Role of circadian rhythm in plant system: An update from development to stress response. *Environmental and Experimental Botany* **162**: 256–271.

Stockinger EJ, Gilmour SJ, Thomashow MF. **1997**. Arabidopsis thaliana CBF1 encodes an AP2 domain-containing transcriptional activator that binds to the C-repeat/DRE, a cis-acting DNA regulatory element that stimulates transcription in response to low temperature and water deficit. *Proceedings of the National Academy of Sciences* **94**: 1035–1040.

Suzuki M, Ketterling MG, McCarty DR. **2005**. Quantitative statistical analysis of cis-regulatory sequences in ABA/VP1- and CBF/DREB1-regulated genes of Arabidopsis. *Plant Physiology* **139**: 437–447.

Thines B, Harmon FG. **2010**. Ambient temperature response establishes ELF3 as a required component of the core Arabidopsis circadian clock. *Proceedings of the National Academy of Sciences of the United States of America* **107**: 3257–3262.

Ulker B, Somssich IE. **2004**. WRKY transcription factors: from DNA binding towards biological function.

Current Opinion in Plant Biology **7**: 491–498.

Wai CM, Weise SE, Ozersky P, Mockler TC, Michael TP, VanBuren R. **2019**. Time of day and network reprogramming during drought induced CAM photosynthesis in Sedum album. *PLoS Genetics* **15**: e1008209.

Walter A, Silk WK, Schurr U. **2009**. Environmental effects on spatial and temporal patterns of leaf and root growth. *Annual Review of Plant Biology* **60**: 279–304.

Wang Y, Wu J-F, Nakamichi N, Sakakibara H, Nam H-G, Wu S-H. **2011**. LIGHT-REGULATED WD1 and PSEUDO-RESPONSE REGULATOR9 Form a Positive Feedback Regulatory Loop in the Arabidopsis Circadian Clock. *The Plant Cell* **23**: 486–498.

Warnes GR, Bolker B, Bonebakker L, Gentleman R, Liaw WHA, Lumley T, Maechler M, Magnusson A, Moeller S, Schwartz M, *et al.* 2019. gplots: Various R Programming Tools for Plotting Data.

Watts WR. **1971**. Role of temperature in the regulation of leaf extension in *Zea mays*. *Nature* **229**: 46–47.

Weigel D, Glazebrook J. **2006**. Root transformation of Arabidopsis. *CSH Protocols* **2006**.

Wickham H. **2016**. ggplot2: Elegant Graphics for Data Analysis.

Wickham H, François R, Henry L, Müller K. **2019**. dplyr: A Grammar of Data Manipulation.

Winter D, Vinegar B, Nahal H, Ammar R, Wilson GV, Provart NJ. **2007**. An electronic fluorescent pictograph browser for exploring and analyzing large-scale biological data sets. *PloS One* **2**: e718.

Wood SN. **2004**. Stable and efficient multiple smoothing parameter estimation for generalized additive models. *Journal of the American Statistical Association* **99**: 673–686.

Wu G, Anafi RC, Hughes ME, Kornacker K, Hogenesch JB. **2016a**. MetaCycle: an integrated R package to evaluate periodicity in large scale data. *Bioinformatics* **32**: 3351–3353.

Wu J-F, Tsai H-L, Joanito I, Wu Y-C, Chang C-W, Li Y-H, Wang Y, Hong JC, Chu J-W, Hsu C-P, *et al.* 2016b. LWD–TCP complex activates the morning gene CCA1 in Arabidopsis. *Nature Communications* **7**.

Xie Q, Wang P, Liu X, Yuan L, Wang L, Zhang C, Li Y, Xing H, Zhi L, Yue Z, *et al.* 2014. LNK1 and LNK2 are transcriptional coactivators in the Arabidopsis circadian oscillator. *The Plant Cell* **26**: 2843–2857.

Yang R, Su Z. **2010**. Analyzing circadian expression data by harmonic regression based on autoregressive spectral estimation. *Bioinformatics* **26**: i168–74.

Yeom M, Kim H, Lim J, Shin A-Y, Hong S, Kim J-I, Nam HG. **2014**. How do phytochromes transmit the light quality information to the circadian clock in Arabidopsis? *Molecular Plant* **7**: 1701–1704.

Zdepski A, Wang W, Priest HD, Ali F, Alam M, Mockler TC, Michael TP. **2008**. Conserved Daily Transcriptional Programs in Carica papaya. *Tropical Plant Biology* **1**: 236–245.

Zhang R, Podtelezhnikov AA, Hogenesch JB, Anafi RC. **2016**. Discovering Biology in Periodic Data through Phase Set Enrichment Analysis (PSEA). *Journal of Biological Rhythms* **31**: 244–257.

Zoltowski BD, Imaizumi T. **2014**. Structure and Function of the ZTL/FKF1/LKP2 Group Proteins in Arabidopsis. *The Enzymes* **35**: 213–239.

SUPPORTING INFORMATION

Fig. S1. Distribution of read counts per time point between conditions.
Fig. S2. Distribution of Metacycle p-value assignments across conditions.
Fig. S3. Relative expression of suggested controls for single-gene PCR quantitation.
Fig. S4. Phylogenetic analysis of *A. thaliana RVE* genes *AtRVE6* and *AtRVE8*.
Fig. S5. Phylogenetic analysis of *A. thaliana LWD* genes, *AtLWD1* and *AtLWD2*.
Fig. S6. Phylogenetic analysis of *A. thaliana LNK* genes *AtLNK1* and *AtLNK2*.
Fig. S7. Heatmap showing z-score normalized expression of all transcripts expressed in all four conditions, segregated into hierarchical clusters.
Fig. S8. Gene ontology terms overrepresented in each phase across the four conditions.
Fig. S9. Heatmap of significant 3-8 bp elements across conditions.
Fig. S10. Complete list of cis-regulatory sequences overrepresented for each phase in each of the conditions.
Fig. S11. Non-redundant set of enriched DAP-seq motifs and highest likelihood *A. thaliana* transcription factor matches.
Table S1. Total number of trimmed reads and percent mapped for each sequenced library.
Table S2. Protein sequences used for phylogenetic analysis.
Table S3. List of previously recommended control genes for single-gene PCR quantitation and their associated coefficient of variance.
Table S4. List of nine *B. distachyon* transcripts with minimal expression change between conditions or time points.
Table S5. List of *B. distachyon* circadian clock genes and their *A. thaliana* ortholog, along with associated period and phase.
Table S6. Summary of pairwise Wilcoxon rank sum significance tests performed for period length comparisons.
Table S7. Summary of pairwise Wilcoxon rank sum significance tests performed for relative amplitude comparisons.

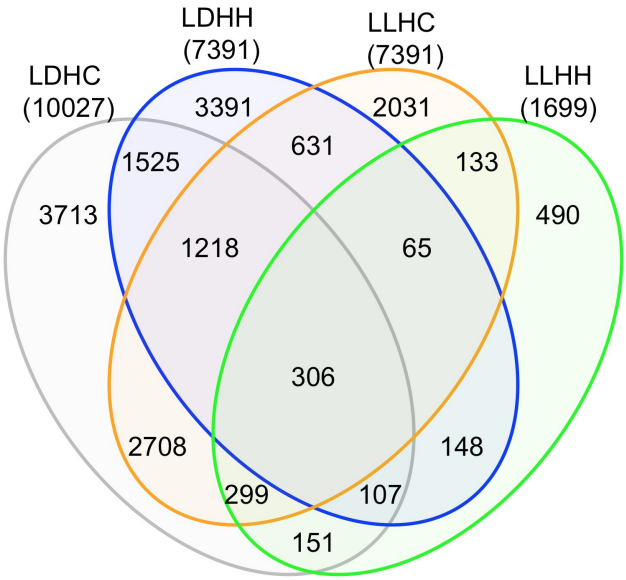

Figure 1. 30% of the *Brachypodium distachyon* transcriptome is controlled by photocycles, thermocycles, or the circadian clock. Venn diagram of the number of transcripts determined to be rhythmic by MetaCycle using a p-value cutoff of < 0.01. Each value within the ovals is the count of rhythmic transcripts exclusive to each union. Total numbers of transcripts measured as rhythmic in each condition are in parentheses. LDHC, photo- and thermocycles; LDHH, photocycles and constant temperature; LLHC, thermocycles and constant light; LLHH, constant light and constant warm temperature.

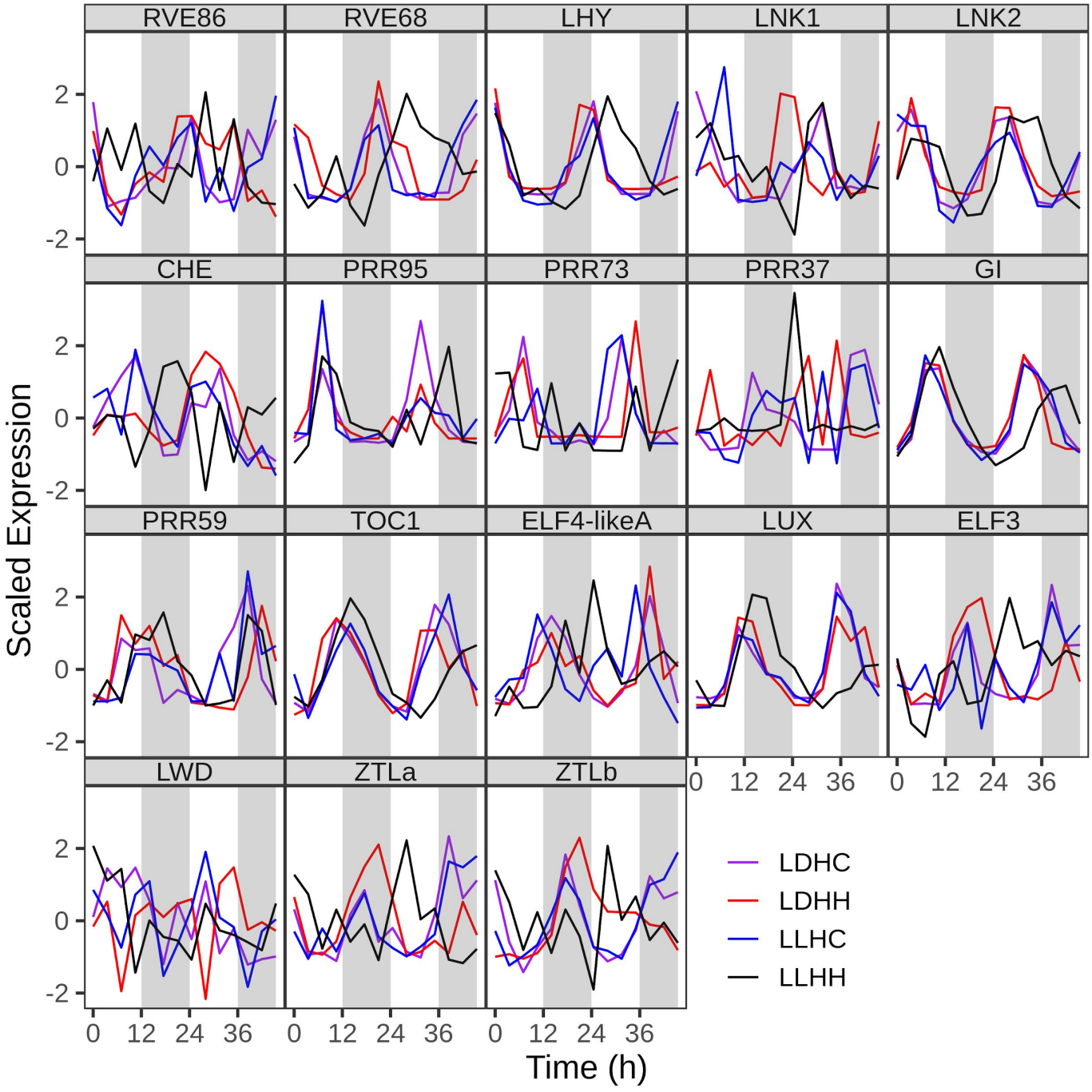

Figure 2. Scaled expression of putative *Brachypodium distachyon* core circadian clock genes in the four time course conditions. Time course names are as described for Figure 1. Source of *B. distachyon* gene identification is described in Supporting Information Table 2.

a.

b.

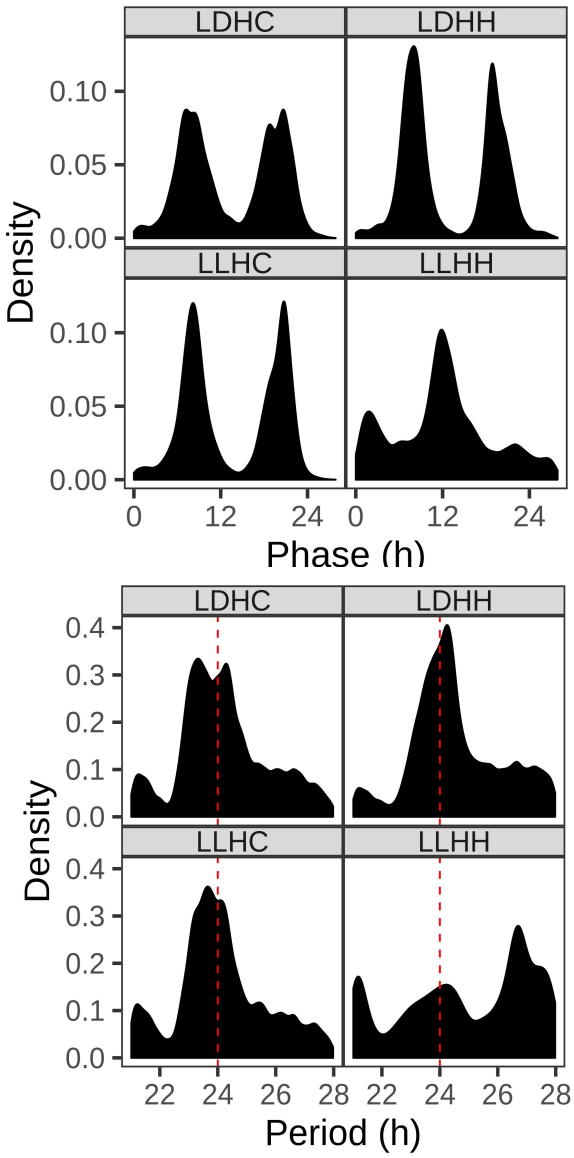

Figure 3. The phase and period of gene expression were primarily conserved in the presence of external cues with a large shift in constant conditions. Distribution of the **(A)** point of maximal expression (phase) and **(B)** period length of cycling transcripts for each condition as determined by MetaCycle. Time course names are as described for Figure 1.

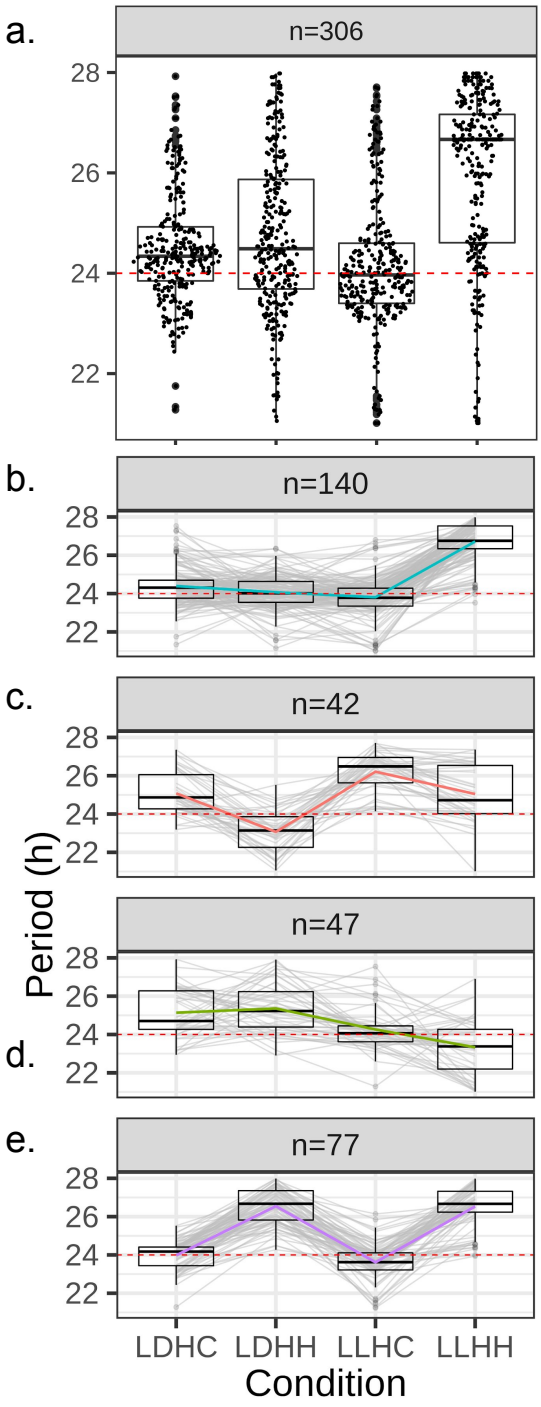

Figure 4. The period length of transcripts rhythmic in all four conditions (a). The period length of the 306 circadian clock-regulated transcripts with a significant period between 21 and 28 h under all four conditions is overlaid on a boxplot to denote the interquartile range of the period data. Each line represents a unique transcript and its period within a condition. Hierarchical clustering was done on normalized period data to group the transcripts into four unique clusters (b-e); n is the number of transcripts in each cluster. The boxes represent the interquartile range, the median value is depicted by a black line, and whisker length is determined as 1.5 times the interquartile range. Time course names are as described for Figure 1.

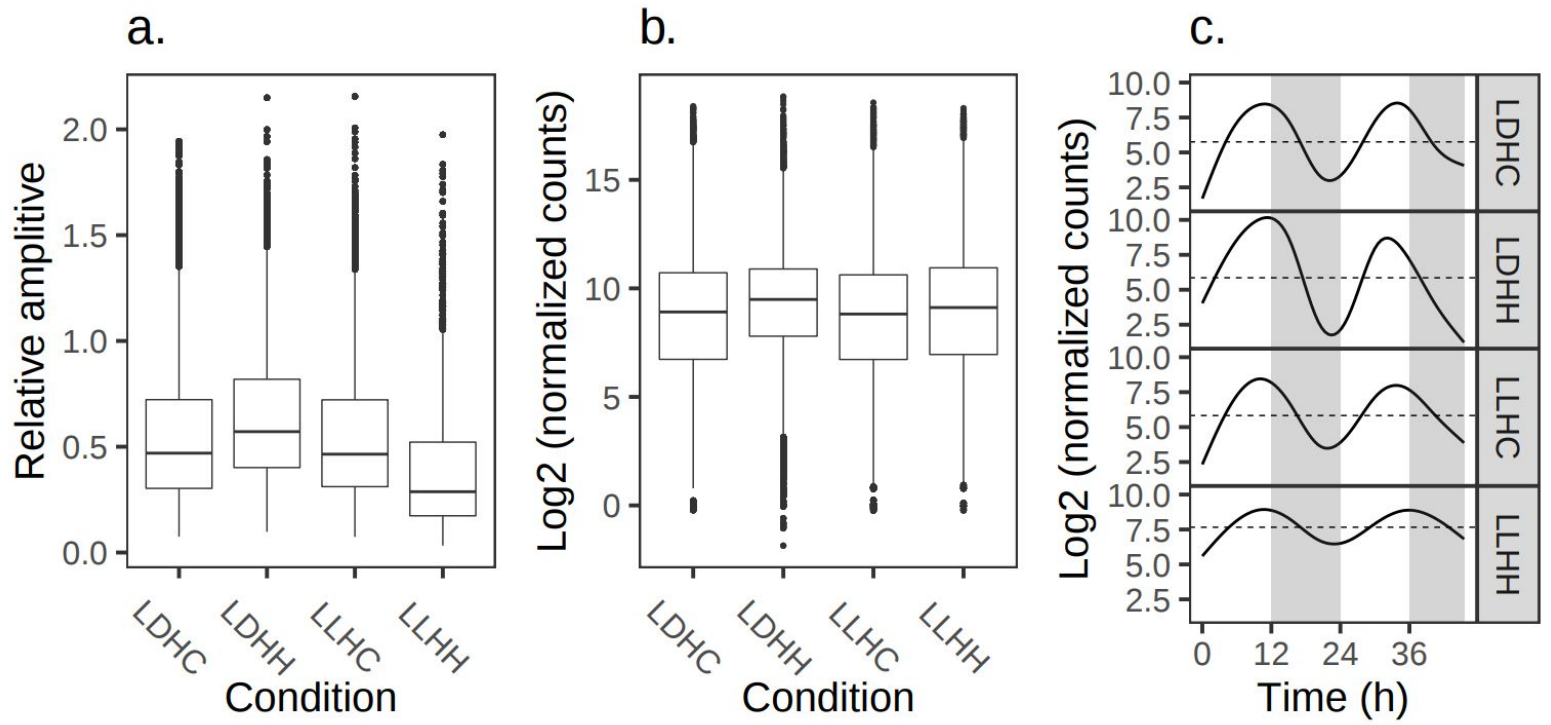

Figure 5. Transcript abundance increased under constant temperatures while photocycles increased relative amplitude. Relative amplitude (**a**) and normalized expression (**b**) of all transcripts rhythmic within each condition. The boxes represent the interquartile range, the median value is depicted by a black line, whisker length is determined as 1.5 times the interquartile range, and outliers are represented by separated dots. (**c**) Representative trendline of all rhythmic transcripts with a phase of approximately 11 h. Is shown to highlight changes in amplitude and expression between conditions. Dotted horizontal line is the mean relative expression level. Box plots and time course names are as described in Figure 1.

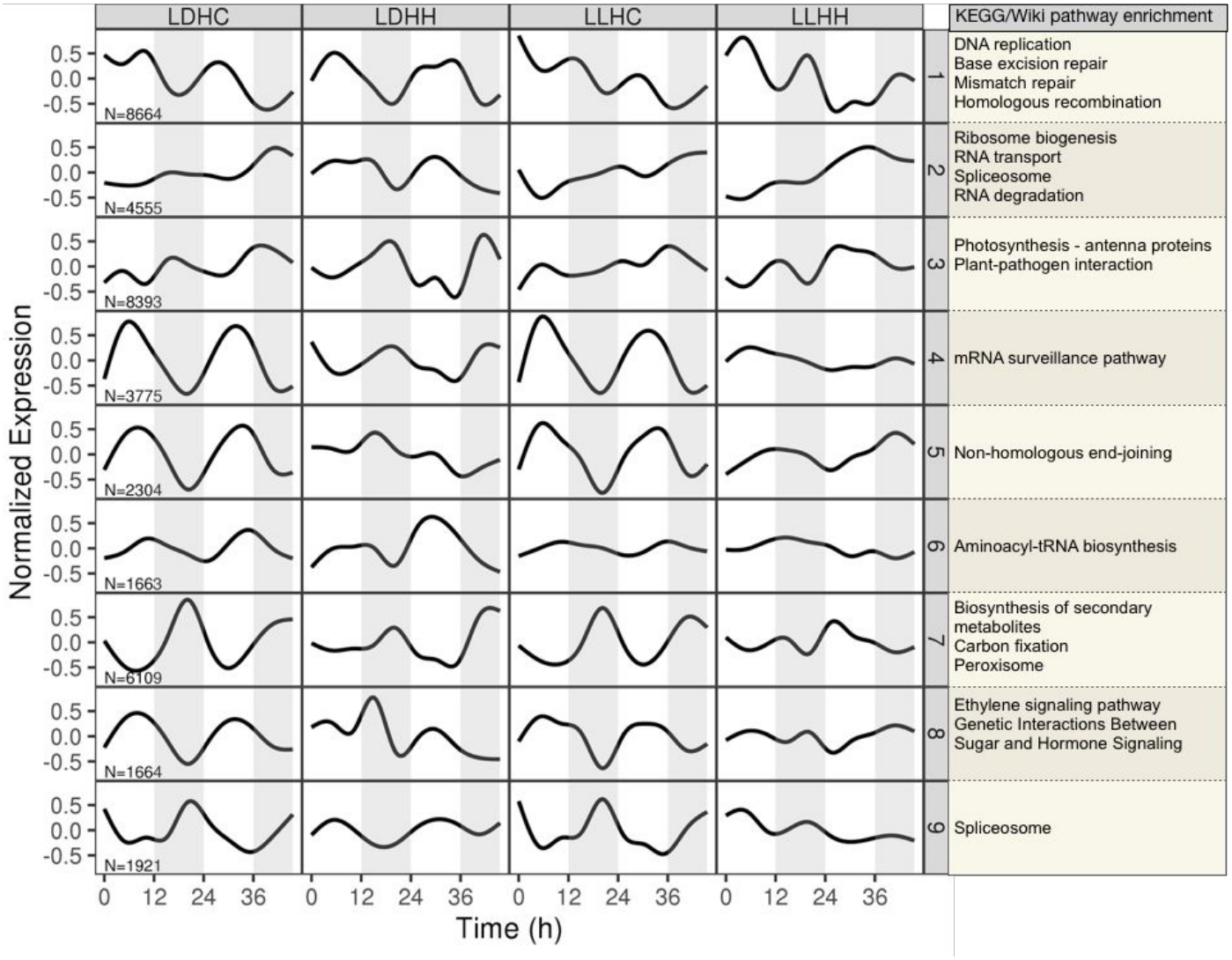

Figure 6. Transcripts associated with specific pathway functions are uniquely or similarly influenced by external cues. Normalized trendline representation of cluster expression by condition along with associated KEGG or Wiki pathway enrichment. Clusters of genes were determined by hierarchical clustering from supporting information fig. 3. Grey rectangles indicate subjective night. N is the number of genes per cluster. Time course names are as described for Figure 1.

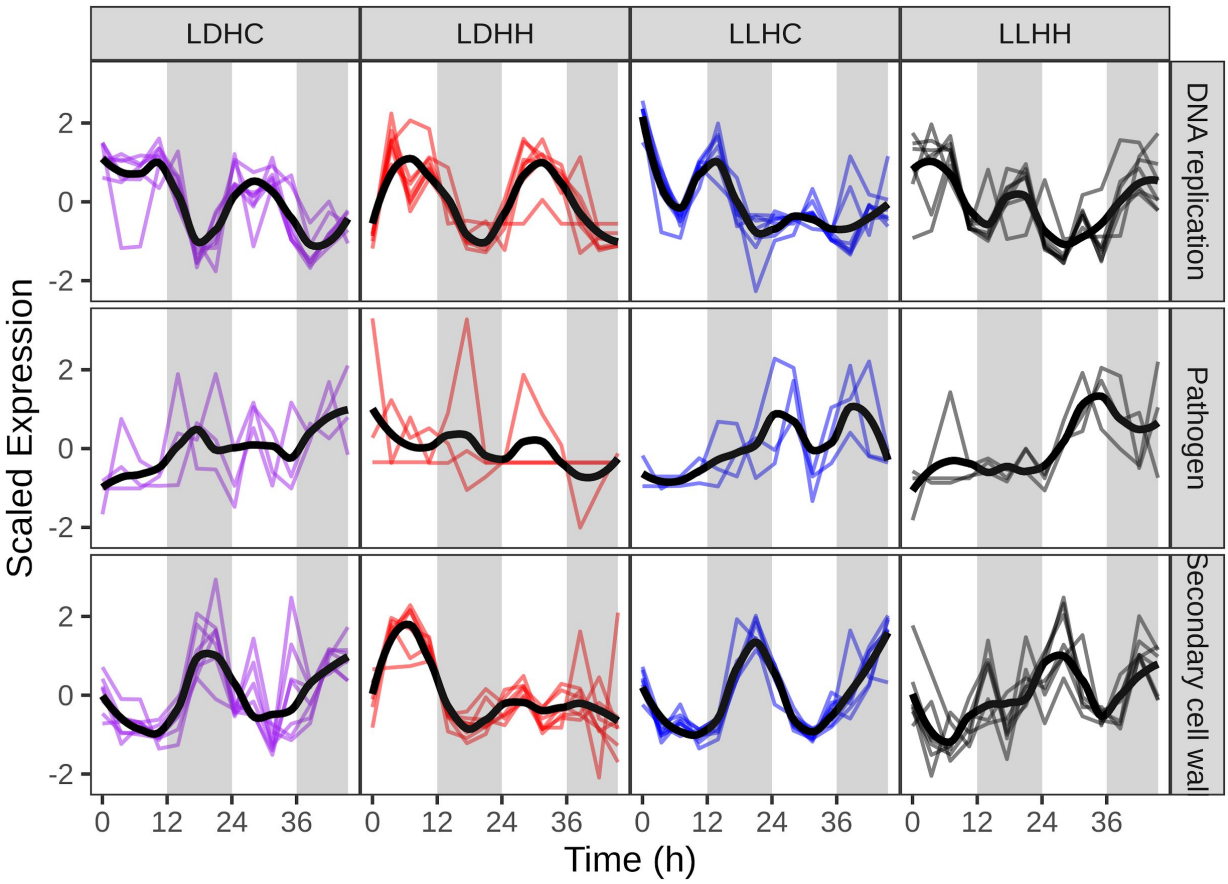

Figure 7. Scaled expression of representative transcripts associated with the given gene ontology term. Black line is the trendline for the transcripts shown. Colored lines are individual transcripts. Gray vertical bars represent subjective night. Time course names are as described for Figure 1.

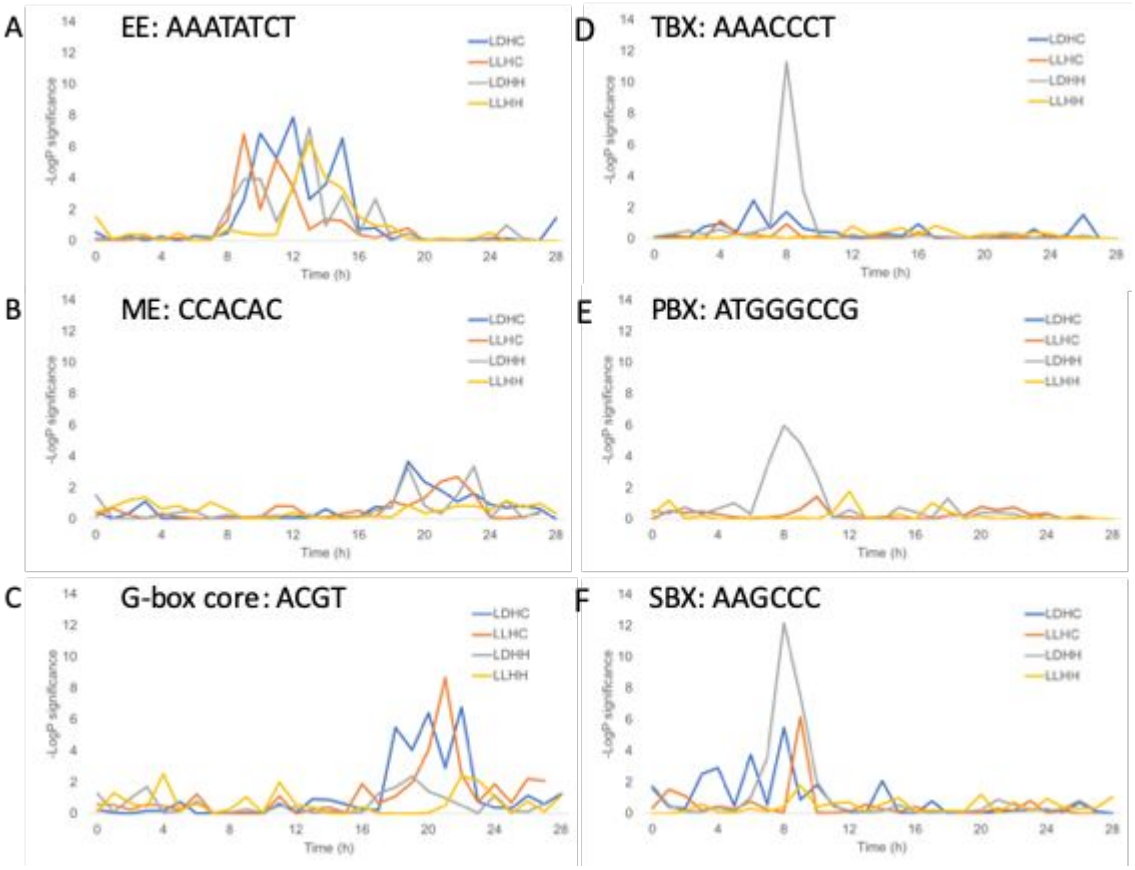

Figure 8. Time-of-day specific diurnal and circadian *cis*-elements. Negative log P values for known diurnal and circadian cis-elements (A) evening element (ME), (B) morning element (ME), (C) G- box core, (D) telobox (TBX), (E) protein box (PBX) and (F) starch box (SBX) were plotted across the day to identify the time of day they were overrepresented in *cis*-regulatory region of genes that cycle with that specific phase. Time course names are as described for Figure 1.

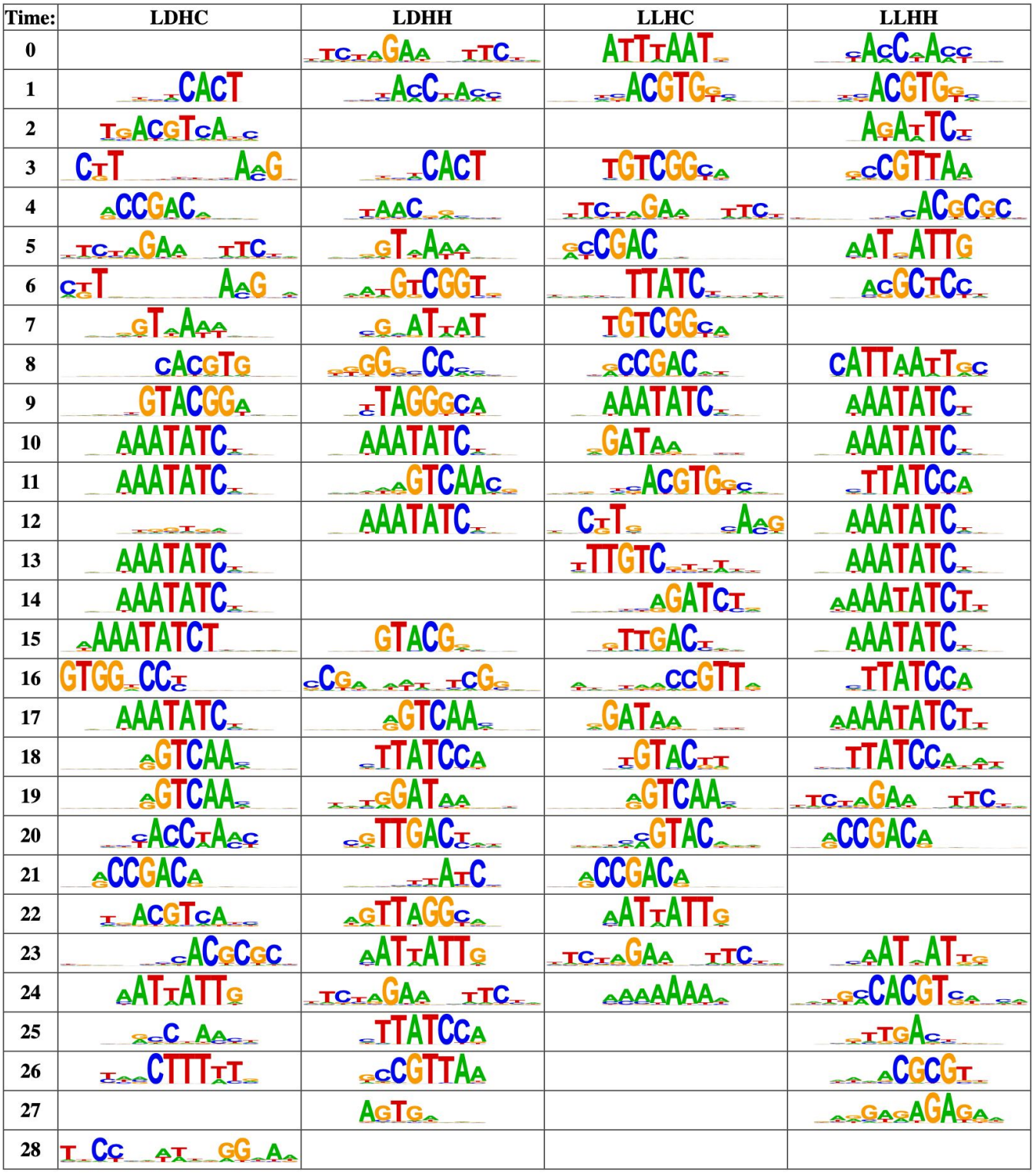

Figure 9. *Cis*-regulatory sequences most overrepresented at each hour in each time course. Each nucleotide sequence is a position probability matrix motif derived from DNA-affinity purification sequencing and identified as enriched in diurnal (LDHC, LDHH, and LLHC) or constant (LLHH) conditions. The height of the letter at each position is proportional to the probability of a given nucleotide. Time course names are as described for Figure 1.